nffa.eu
PILOT 2021 2026

WP11 JA1 - Real-time observation and control in microscopy and spectroscopy of nano-objects

D11.1

Commissioning of HHG with enhanced properties

Due date
M12

PROJECT DETAILS

PROJECT ACRONYM	PROJECT TITLE
NEP	Nanoscience Foundries and Fine Analysis - Europe|PILOT

GRANT AGREEMENT NO:	FUNDING SCHEME
101007417	RIA - Research and Innovation action

START DATE

01/03/2021

WORK PACKAGE DETAILS

WORK PACKAGE ID	WORK PACKAGE TITLE
WP 11	Real-time observation and control in microscopy and spectroscopy of nano-objects

WORK PACKAGE LEADER

Prof. Giovanni De Ninno (UNG)

DELIVERABLE DETAILS

DELIVERABLE ID	DELIVERABLE TITLE
D11.1	Commissioning of HHG with enhanced properties.

DELIVERABLE DESCRIPTION

Implementation of schemes producing HHG light with short pulses and high degree of circular polarization

DUE DATE	ACTUAL SUBMISSION DATE
12 (Month) 28/02/2022	16/02/2022

AUTHORS

Paraskevas Tzallas (FORTH), Emmanuel Stratakis (FORTH), Giovanni De Ninno (UNG), Carlo Spezzani (UNG)

PERSON RESPONSIBLE FOR THE DELIVERABLE

Emmanuel Stratakis (FORTH), Giovenni De Ninno (UNG)

NATURE

☐   R - Report

☒   P - Prototype, Demonstrator

☐   DEC - Websites, Patent filing, Press & media actions, Videos, etc

☐   O - Other

DISSEMINATION LEVEL

☒   P - Public

☐   PP - Restricted to other programme participants & EC: (Specify)

☐   RE - Restricted to a group   (Specify)

☐   CO - Confidential, only for members of the consortium

REPORT **DETAILS**

VERSION	DATE	AUTHOR(S)	DESCRIPTION / REASON FOR MODIFICATION	STATUS
1	16/02/2022			Draft
				Choose an item.
				Choose an item.
				Choose an item.

CONTENTS

INTRODUCTION

During the first year of NEP project the beam line towards the generation of intense circularly polarized XUV radiation was under development and implementation. The two techniques for the generation of intense circular polarized XUV radiation were installed to the MW beamline based on the Attosecond Science and Technology (AST) Laboratory of IESL-FORTH (see Figure 1). By applying the two-color counter rotating electric fields setup under loose focusing conditions we were able to generate highly elliptical extreme ultraviolet radiation in Ar gas as generating medium (see Figure 2). The energy of the XUV radiation emitted per laser pulse is found to be of the order of ~100 nJ with the spectrum spanning from 17 to 26 eV (See Figure 3(b)). Preliminary results in Xe and Ne gas as generating medium are also available. Briefly, it was found in Xe that under optimal conditions the energy content of highly elliptical XUV radiation was of the order of the order of ~200 nJ with a spectrum spanning from 17 to 22 eV. On the other hand in the case of Ne as generating medium the energy content was in the order of pJ in the spectral region 17-29 eV.

The current performance of high-harmonic generation sources offers a temporal resolution of a few tens of femtoseconds and an energy resolution of approximately one hundred meV. However, some of the most intriguing open problems in materials science arise from phenomena taking place at faster time-scales, in the few-femtosecond range. This includes physical processes, such as the collapse and recovery of metallic or magnetic states, electron hopping, screening phenomena, or charge transfer mechanisms. During the first year of the project, in order to access such temporal scales by means of time and angular-resolved photo-electron spectroscopy (tr-ARPES), we started to implement an optical setup, which allowed us to generate laser pulses in the sub-10 femtosecond range. The few-cycle pulses have been generated by focusing the driving laser of the CITIUS light source at Nova Gorica university into a capillary wave-guide, placed in an environment filled with noble gas. This induced a proper amount of self-phase modulation, i.e., a controlled increase of the pulse bandwidth. The latter has been then recompressed by means of "chirped" mirrors, designed to introduce a proper amount of dispersion, down to a few femtoseconds.

Experimental progress

High-harmonic generation pulses with circular polarization

The estimation of the energy content of the highly elliptical XUV radiation emitted per pulse is discussed. The estimation was enabled by calibrating the XUV emission in the case of the highly elliptical polarized light with the measured energy in the case of p-polarized XUV radiation. The linear polarized HHG signal was measured with a calibrated XUV photodiode (XUV PD) (Opto Diode AXUV100G) placed on the XUV beam path after the Sn filter. The photodiode signal was measured with the harmonic generation gas jet ON and OFF. The measured signal when the jet was OFF comes from the residual IR radiation and is subtracted from the signal measured when the generation gas was ON. A similar measurement for the highly elliptically polarized radiation has a high degree of uncertainty because the difference of the two signals (gas jet ON − gas jet OFF) is rather small. This is due to significantly increased amount of light of the fundamental as well as of the second harmonic frequencies reflected from the Si plate in the case of not p-polarized fields. Therefore, when MAZEL-TOV-like device is introduced in the beam path for generating highly

elliptical XUV, the driving fields are significantly reflected and the scattered light introduced to the XUV PD is preventing an accurate measurement regarding the HHG signal. Thus, the results of such a measurement will not be presented here, although they are compatible with those discussed below.
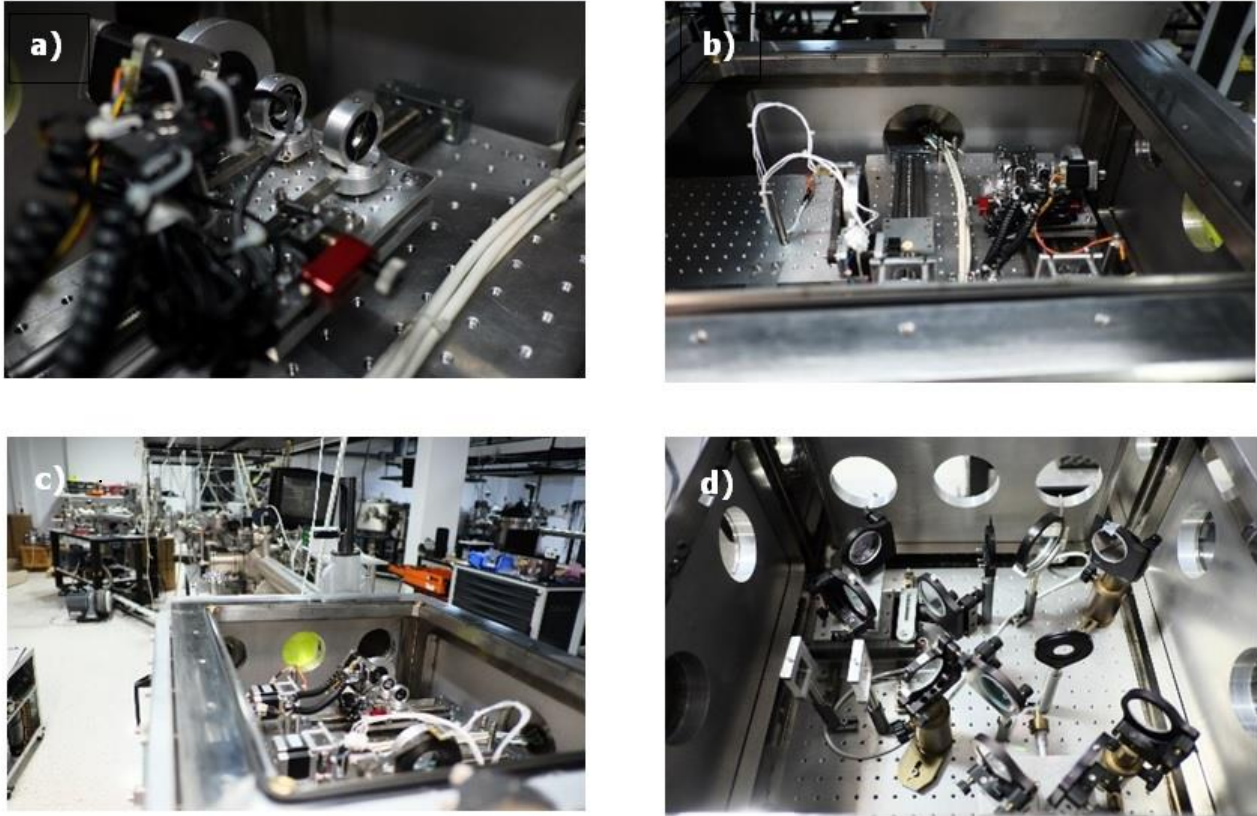

Figure 1: (a), (b), (c) Experimental setup for the generation energetic highly elliptical XUV radiation by two color counter rotating circular polarized electric fields under loose focusing conditions. (d) Experimental setup for the generation highly elliptical XUV radiation by aligned molecules. Both experimental strategies were installed in the MW beamline based on the Attosecond Science and Technology Laboratory, a beamline which is fully characterized and it is also a well-known apparatus.

Instead, in order to deduce an estimation of the amount of XUV photons in the case of highly elliptical light, measurements of the Ar single photon ionization PE spectra induced by linear p-polarized and highly elliptical XUV radiation are directly compared at the same detection conditions, after optimization of harmonic emission in both cases. In Figure 3 the PE spectra in the case of linear and highly elliptical polarization is shown for a) Xe and b) Ar gas.

The calibrated photodiode signal, in the case of linearly polarized XUV radiation, was measured by an oscilloscope with 50 Ω input impedance and the measured trace was integrated. The pulse energy is given by $E_{PD} = \sum_q \frac{n_e \cdot w \cdot h v_q}{n_q} \cdot e$ where q is the harmonic order, n_e is the number of produced photoelectrons, w is the statistical weight of the qth harmonic, $h v_q$ is the harmonic photon energy, n_q is the photodiode quantum efficiency and e is the electron charge. The photoelectron number is given by $n_e = \frac{S_T - S_\omega}{e \cdot R}$ where S_T is the total time integrated photodiode

signal, S_ω is the time integrated photodiode signal when the harmonic generation is OFF, e is the electron charge and R is the oscilloscope impedance. The quantum efficiency of the photodiode as a function of the photon energy is provided by the manufacturing company and it is presented in Figure 4(b).
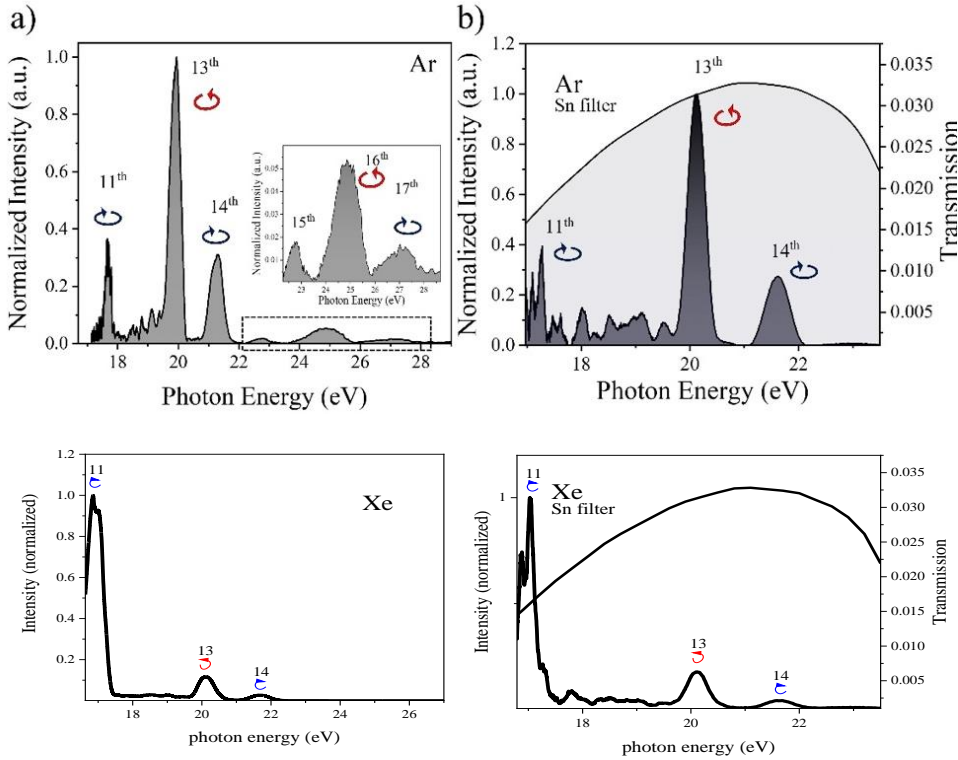

Figure 2: (a), (c) Recorded photoelectron spectra of Argon by the highly elliptical polarized XUV radiation from Ar and Xe as generation media, respectively. (b), (d) HHG spectra transmitted through a 150 nm thick Sn filter for the same generation media and generation conditions.
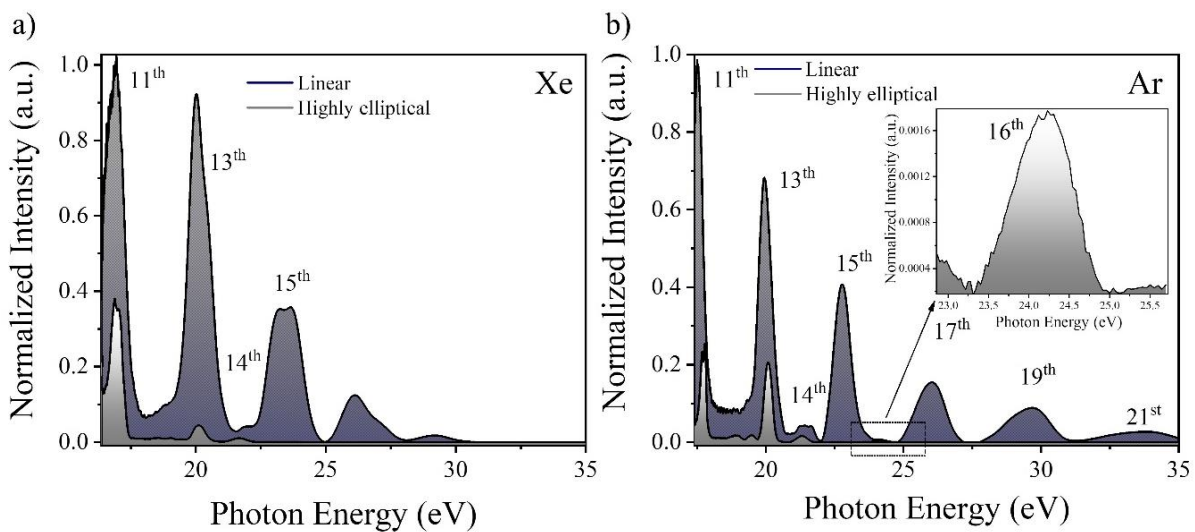

Figure 3: PE spectra of Ar induced by the linear p-polarized and highly elliptical XUV radiation generated by a) Xe and b) Ar, respectively at the same detection conditions, as soon as the optimization of harmonic emission is realized in both cases.

The energy content of the linearly p-polarized XUV radiation was measured when generated in both Xe and Ar. For determining the energy of the harmonic radiation produced in the generation region one has to consider also the filter transmission as well as the Si reflectivity. Then the produced XUV energy E emitted per laser pulse at the harmonic generation source is given by $E = \sum_q \frac{n_e \cdot w \cdot h v_q}{\eta_q \cdot R_q^{Si} \cdot T_q^{Sn}} \cdot e$. Here T_q^{Sn} is the ~3% transmission of the Sn filter in this spectral region measured by recording the harmonic spectrum of linear p-polarized harmonics (with MAZEL-TOV-like device out of the beam path) with and without filter. The main reason that p-polarized XUV radiation was chosen for the callibration of the Sn filter is the higher signal it results with and without the filter thus minimizing the error of the measurement. $R_q^{Si} = 50\% - 60\%$ is reflectivity of the Si plate. Under optimal generation conditions the maximum energies at the source were found to be in the range $E_{Xe}^{linear} \approx 1\mu J - 2\mu J$ and $E_{Ar}^{linear} \approx 0.5\mu J - 1\mu J$. These values concern the emitted 11th,13th,15th ,17th and 19th harmonics laying in the plateau spectral region. Therefore the energy content per harmonic pulse is ~400 nJ and ~200 nJ at the source for Xe and Ar, respectively. In Figure 4 (a) a typical measurement of the p-polarized XUV radiation energy in the case of Xe gas, which corresponds to energy $E_{Xe}^{linear} \approx 2$ µJ at the source is presented.
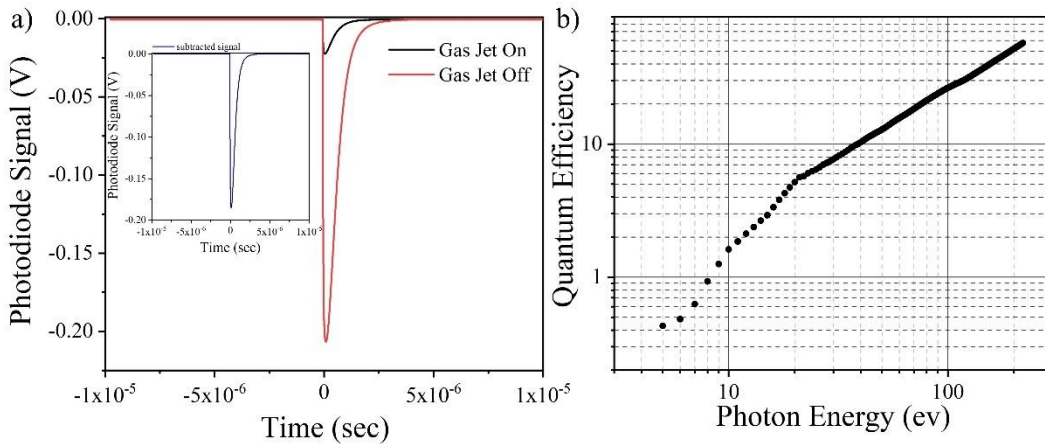

Figure 4: (a) Typical measurement of the p-polarized XUV radiation energy in the case of Xe gas. XUV photodiode signal obtained when HHG switched ON (red line) and with the HHG switched OFF (black line). (b) XUV photodiode quantum efficiency as a function of photon energy provided by the manufacturing company Opto Diode Corp..

Having determined the energy values in the case of linear polarized XUV field and having deduced also the ratios of the harmonic amplitudes in the case of p-polarization and highly elliptical XUV radiation ,by the recordings of the PE spectra, one can extract the energy content of the later one. Particularly, in the case of Xe as the generating medium, the ratio of the integral values $I_q^{highlyelliptical}/I_q^{linear}$,(where q is the harmonic order) was found 0.26, 0.03, and 0.006 for the 11th,13th and 14th harmonics ,respectively. For the generation in Argon the ratio of the similar integral values was found 0.15, 0.17, 0.02, 0.006 for the 11th,13th ,14th and 16th harmonic, respectively. This ratio of the integral values of the two different PE spectra (highly elliptical vs linearly polarized) equals to the ratio of the energy content per harmonic order per laser pulse $I_q^{highlyelliptical}/I_q^{linear} = E_q^{highlyelliptical}/E_q^{linear}$ and has to be divided by the correction parameter ~0.6 introduced by the different percentage of the total photoelectons' number entering the TOF spectrometer. This consideration has to be taken into account due to the different angular

8

photoelectron distributions resulting from the single photon ionization by the two polarization's states (linear, circular). After this correction, the energy per laser pulse emitted in the case of highly elliptical radiation was then estimated to be $E_{Xe}^{highlyelliptical} \approx 200$ nJ and $E_{Ar}^{highlyelliptical} \approx 100$ nJ respectively. It has to be pointed out, that in the case of Xe gas as the generating medium 80 % of the energy is contained in the 11th harmonic and the rest 20% in 13th,14th harmonics while in the case of Ar the energy is almost equally distributed between 11th and 13th harmonics and a small percentage in 14th and 16th harmonics. Conclusively, the energy of highly elliptically polarized XUV radiation is ~10 times less as compared to linearly polarized XUV radiation at the same spectral region, under conditions where the yield was optimized in both cases. The number of photons per harmonic order per pulse is presented in Figure 5.
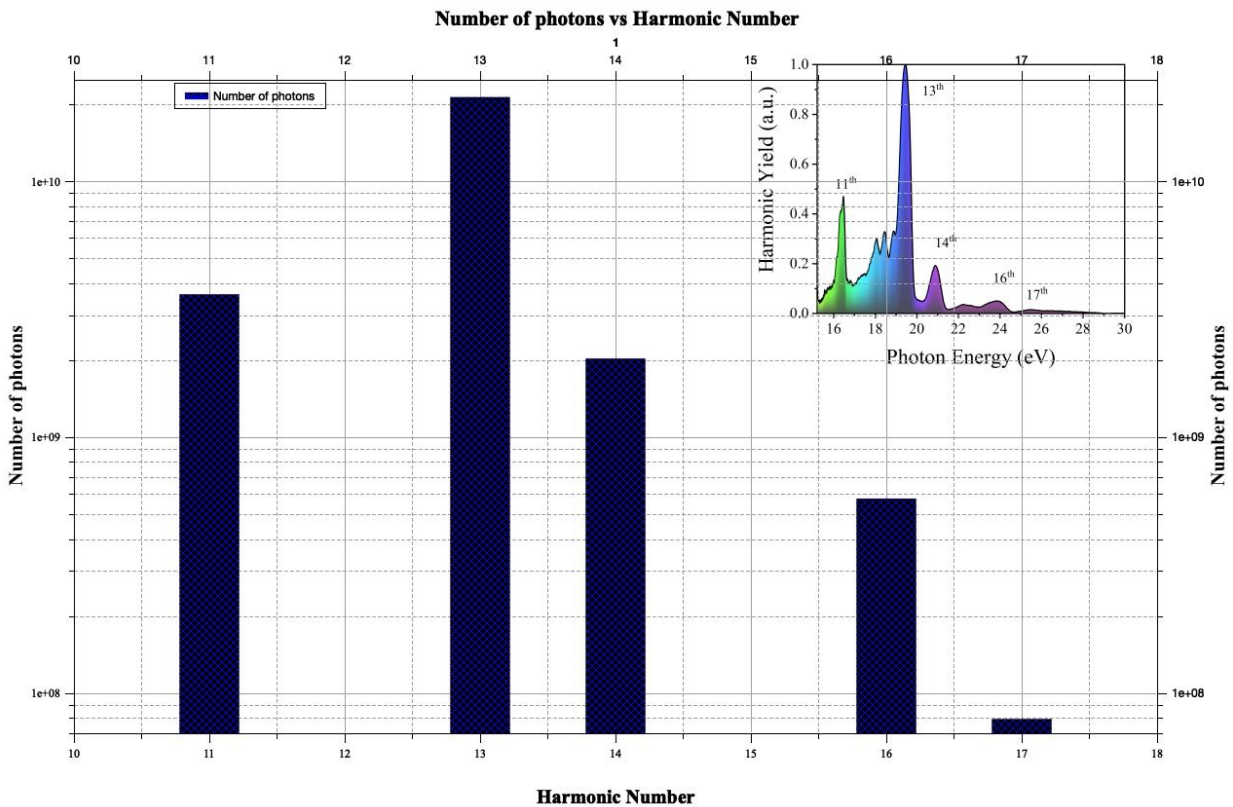

Figure 5: Number of photons per harmonic order per pulse in the case of Ar as generating medium.

The demonstrated energy values (along with tight XUV focusing geometries) are sufficient to induce nonlinear processes. Our results challenge current perspectives regarding ultrafast investigations of chiral phenomena in the XUV spectral region.

Moreover, emphasis should be given to the fact that the harmonic ellipticity and helicity can be fully controlled at the source by simply rotating the fast axis of the super achromatic waveplate. This is based on the conservation of spin angular momentum in HHG process. The equation characterizing the ellipticity for the emitted harmonics allowed by the selection rules as a function of the angle α of the fast axis of the super achromatic waveplate in the case of MAZEL-TOV-like device can be extracted from: $\varepsilon_{n_1,n_2} = \frac{1-\sqrt{1-(n_1-n_2)^2 sin^2(2\alpha)}}{(n_1-n_2)sin(2\alpha)}$ where ε_{n_1,n_2} is the ellipticity of the n_1, n_2 harmonic channel where $n_2 = n_1 \pm 1$. Figure 6(a) presents the estimated harmonic ellipticity

ε_{n_1,n_2} as a function of the rotation angle α of the super achromatic waveplate in our MAZEL-TOV-like device installed in the MW beamline of AST at FORTH-IESL. Figure 6(b) shows the normalized experimental PE spectra as a function of the angle α of the fast axis of the waveplate in the case of Xe as generating medium.
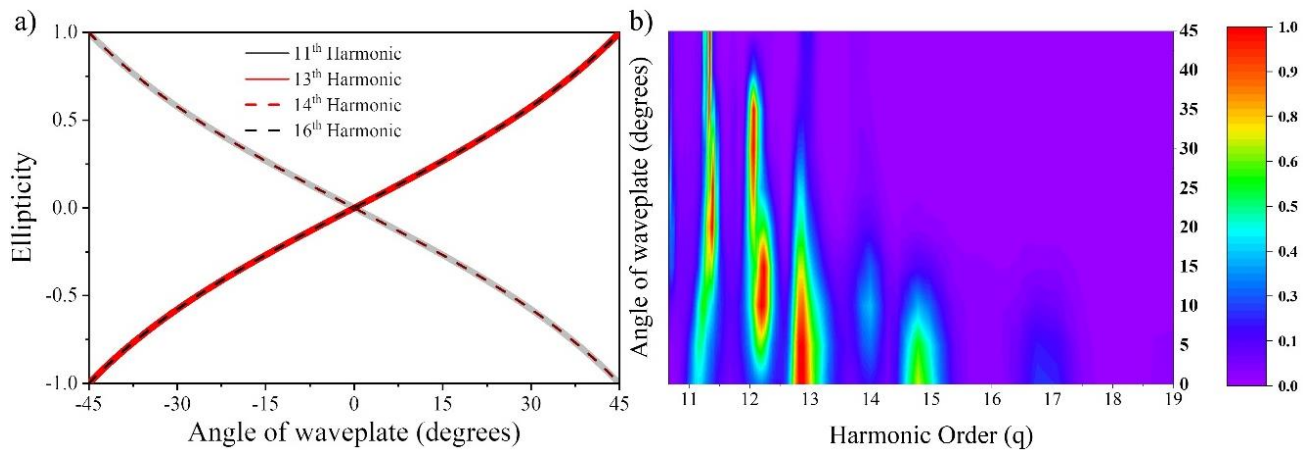

Figure 6: (a) Theoretically predicted ellipticity ε of harmonics 11th, 13th, 14th ,16th generated in an isotropic medium as a function of the angle α of the super achromatic waveplate's fast axis (see text). (b) Normalized PE spectra as a function of the angle α of the fast axis of the waveplate in the case of Xe.

By following fundamental selection rules, it is well known that the generated XUV radiation is highly elliptical polarized. Additionally, a measurement of the polarization state would be complementary. Therefore, in the MW beam line of AST an end station for the characterization of the harmonic ellipticity was developed and installed (Please refer to pictures in Figure 7). The XUV polarizer consists of three mirrors at grazing incidence with different reflectivity for s and p polarization. By rotating this set of mirrors and recording the spectrum with a spectrometer we can analyse the polarization state of the emitted XUV radiation. This project is in progress.

This new beamline developed in AST has unique characteristics. It provides the generation highly elliptical XUV radiation (17-26 eV) with the possibility of controlled polarization, reaching energies per pulse at the range of 100 nJ. A manuscript describing the unique characteristics of this beamline is already published (Vassakis, Emmanouil, Ioannis Orfanos, Ioannis Liontos, and Emmanouil Skantzakis. 2021. "Generation of Energetic Highly Elliptical Extreme Ultraviolet Radiation" Photonics 8, no. 9: 378. https://doi.org/10.3390/photonics8090378).

Finally, according to calculations based on Strong Field Approximation the spectral characteristics of the generated XUV radiation can be controlled by tuning the central wavelength of the second harmonic. This can be succeeded experimentally by simply changing the angle of the BBO crystal compare to the propagation axis of the 25-fs IR pulse. Preliminary results of the calculations are presented in Figure 8.
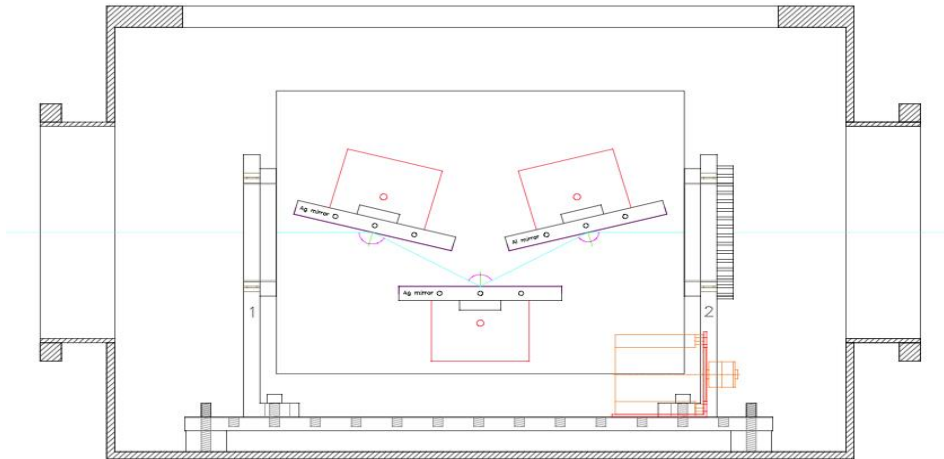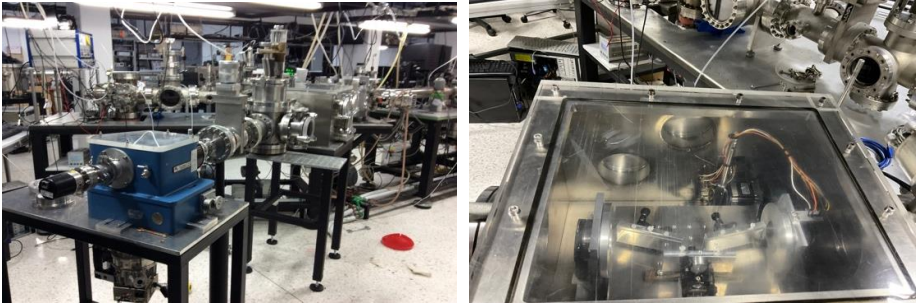
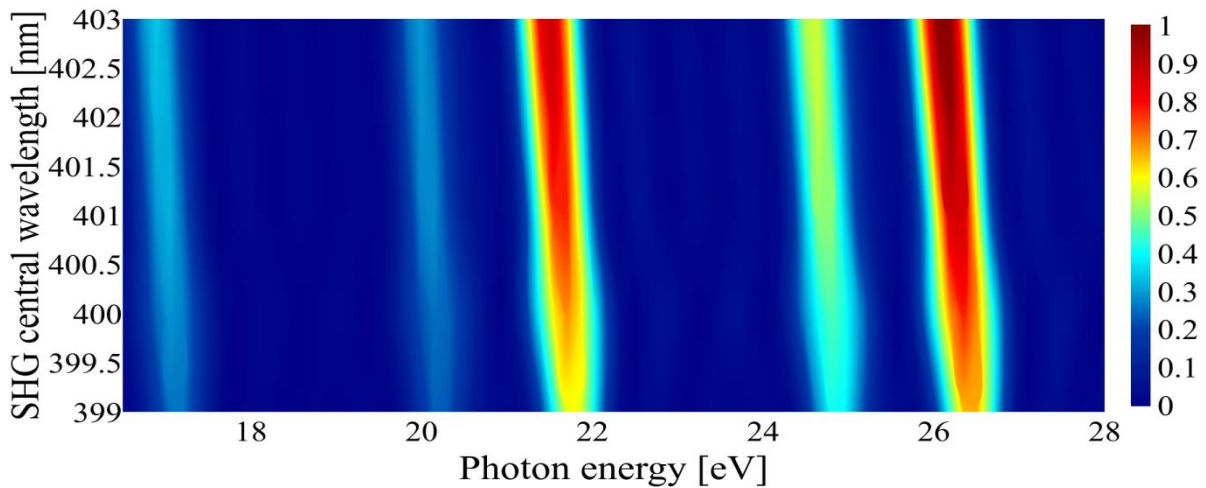Figure 7: XUV polarimetry end station developed in MW beamline of AST Laboratory IESL-FORTH.

Figure 8: Harmonic spectra as a function of photon energy for different SHG central wavelengths (theoretical calculations).

Generation of ultra-short pulses

Figures 9 and 10 show a schematic and a photo of the optical setup that was used to generate ultra-short laser pulses at the CITIUS facility respectively.
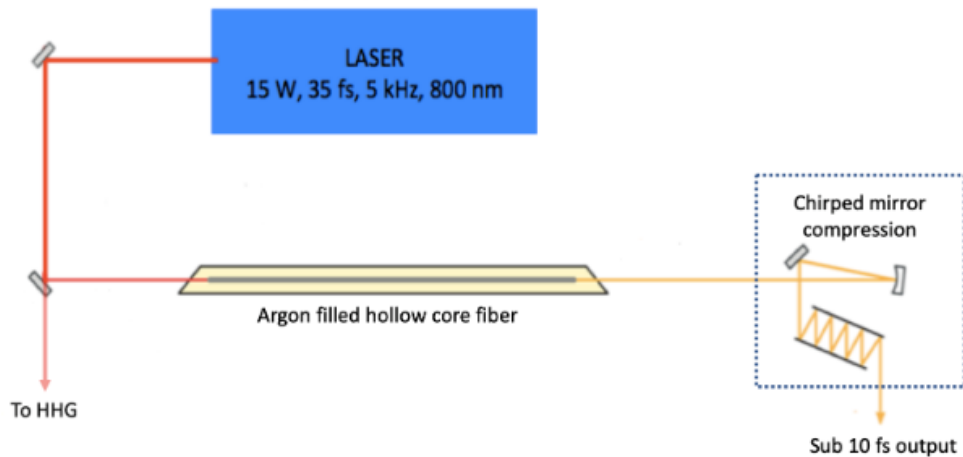

Figure 9: sketch of the hollow fibre compressor set-up at CITIUS light source. The light is focussed into a hollow fibre filled with argon. The output of the fibre is compressed using an array of chirped mirrors.
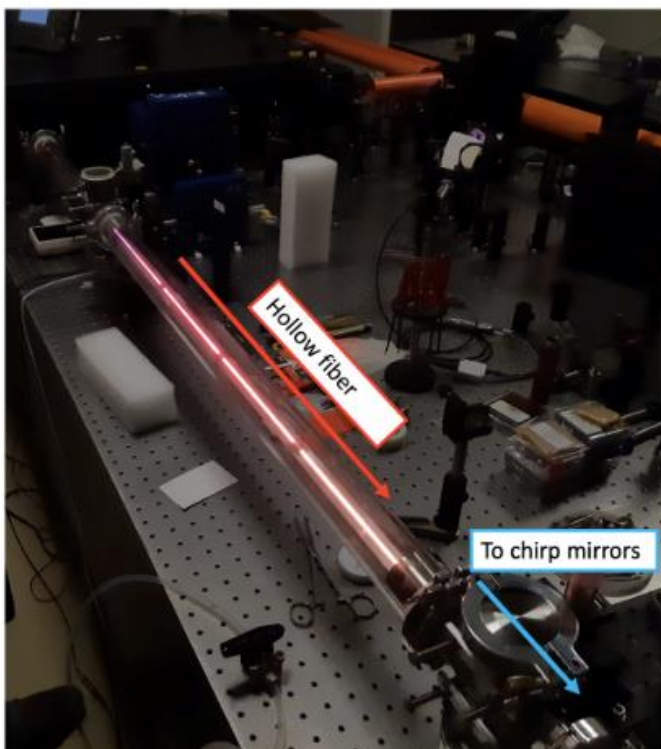

Figure 10: Image of the hollow fibre compressor at the CITIUS light source. As the pulse propagates through the fibre it experiences self-phase modulation, the consequent broadening of the optical bandwidth leads to a generation of "super-continuum" or "white light".

We used the ultra-short laser pulses for an experiment aimed at dissecting Mott and charge-density wave dynamics in the photo-induced phase of a sample of 1T-TaS2.

The two-dimensional transition-metal dichalcogenide 1T-TaS2 is a complex material standing out for its puzzling low temperature phase marked by signatures amenable to both Mott-insulating and charge-density wave states. Electronic Mott states, coupled to a lattice, respond to coherent optical excitations via a modulation of the lower (valence) Hubbard band. Such dynamics is driven by strong electron-phonon coupling and typically lasts for tens of picoseconds, mimicking coherent structural distortions. Instead, the response occurring at the much faster timescale, mainly dominated by electronic many-body effects, is still a matter of intense research. By performing tr-ARPES, we investigated the photo-induced phase of 1T-TaS2 and found out that its lower Hubbard band promptly reacts to coherent optical excitations by shifting its binding energy towards a slightly larger value. This process lasts for a time comparable to the optical pump pulse length, mirroring a transient change of the onsite Coulomb repulsion energy (Figure 11).
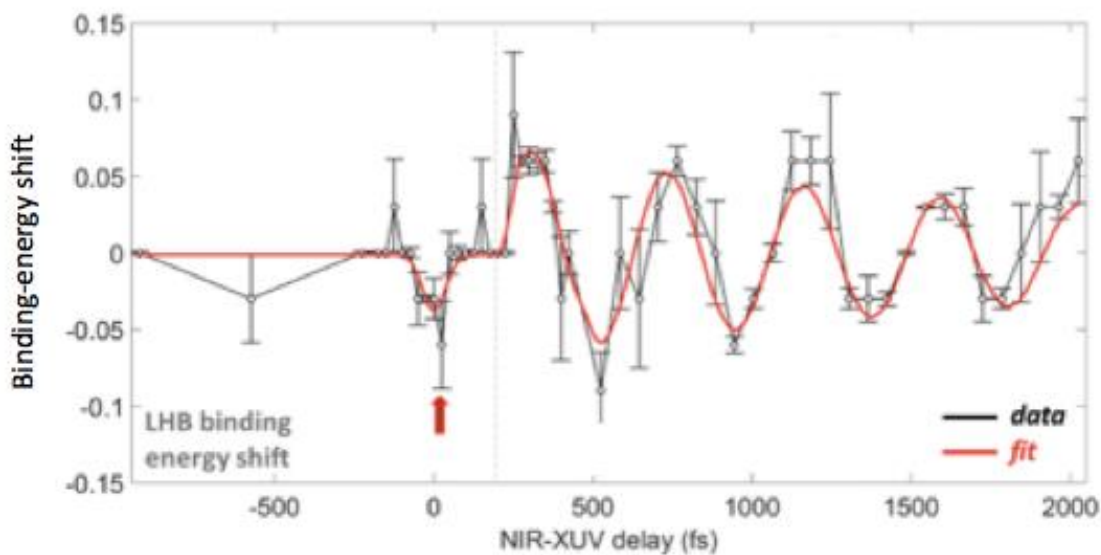

Figure 11: Binding-energy shift time trace (black dots) in a sample of TaS2. The red arrow is a guide for the eyes to mark the prompt responses that was detected using the ultra-fast pump pulse generated at CITIUS. The red line has been obtained using a fit function.